

AD-A144 713

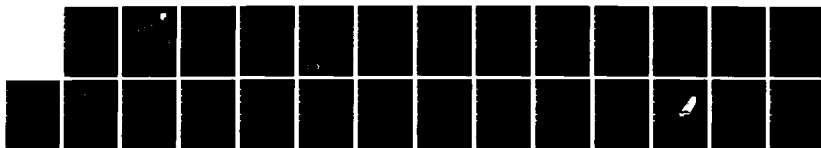
ENERGY DEPOSITION IN MICROVOLUMES OF SILICON FROM HIGH  
ENERGY PROTON REACTIONS(U) ROME AIR DEVELOPMENT CENTER  
GRIFFISS AFB NY J N BRADFORD FEB 84 RADC-TR-84-5

1/1

UNCLASSIFIED

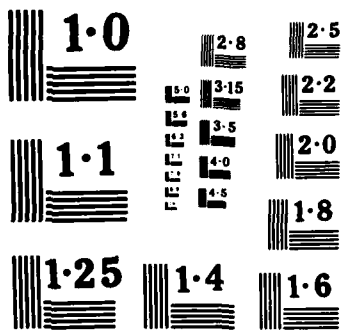
F/G 28/12

NL



END

FILMED  
-  
DTIC



12

**RADC-TR-84-5**  
**In-House Report**  
**February 1984**



**AD-A144 713**

# ***ENERGY DEPOSITION IN MICROVOLUMES OF SILICON FROM HIGH ENERGY PROTON REACTIONS***

**John N. Bradford**

**DTIC**  
**ELECTE**  
**AUG 21 1984**  
**S**  
**B**

**APPROVED FOR PUBLIC RELEASE; DISTRIBUTION UNLIMITED**

**ROME AIR DEVELOPMENT CENTER**  
**Air Force Systems Command**  
**Griffiss Air Force Base, NY 13441**

**DTIC FILE COPY**

**84 08 20 157**

This report has been reviewed by the RADC Public Affairs Office (PA) and is releasable to the National Technical Information Service (NTIS). At NTIS it will be releasable to the general public, including foreign nations.

RADC-TR-84-5 has been reviewed and is approved for publication.

APPROVED:

*Bobby L. Buchanan*

BOBBY L. BUCHANAN, Chief  
Radiation Hardened Elect Technology Branch

APPROVED:

*Harold Roth*

HAROLD ROTH, Director  
Solid State Sciences Division

FOR THE COMMANDER:

*John A. Ritz*

JOHN A. RITZ  
Acting Chief, Plans Office

If your address has changed or if you wish to be removed from the RADC mailing list, or if the addressee is no longer employed by your organization, please notify RADC (ESR) Hanscom AFB MA 01731. This will assist us in maintaining a current mailing list.

Do not return copies of this report unless contractual obligations or notices on a specific document requires that it be returned.

Unclassified

SECURITY CLASSIFICATION OF THIS PAGE

| REPORT DOCUMENTATION PAGE  |  |  |  |            |                 |
|--|--|--|--|------------|-----------------|
| 1a REPORT SECURITY CLASSIFICATION<br>Unclassified  |  | 1b RESTRICTIVE MARKINGS  |  |            |                 |
| 2a SECURITY CLASSIFICATION AUTHORITY   |  | 3 DISTRIBUTION/AVAILABILITY OF REPORT<br><br>Approved for public release;<br>distribution unlimited. |  |            |                 |
| 2b DECLASSIFICATION/DOWNGRADING SCHEDULE   |  |  |  |            |                 |
| 4 PERFORMING ORGANIZATION REPORT NUMBER(S)<br><br>RADU-TR-84-5   |  | 5 MONITORING ORGANIZATION REPORT NUMBER(S)   |  |            |                 |
| 6a NAME OF PERFORMING ORGANIZATION<br>Rome Air Development<br>Center   | 6b OFFICE SYMBOL<br>(If applicable)<br>ESR | 7a NAME OF MONITORING ORGANIZATION   |  |            |                 |
| 6c ADDRESS (City, State and ZIP Code)<br>Hanscom AFB<br>Massachusetts 01731  |  | 7b ADDRESS (City, State and ZIP Code)  |  |            |                 |
| 8a NAME OF FUNDING/SPONSORING<br>ORGANIZATION<br>Rome Air Development Center   | 8b OFFICE SYMBOL<br>(If applicable)<br>ESR | 9 PROCUREMENT INSTRUMENT IDENTIFICATION NUMBER   |  |            |                 |
| 8c ADDRESS (City, State and ZIP Code)<br>Hanscom AFB<br>Massachusetts 01731  |  | 10 SOURCE OF FUNDING NOS   |  |            |                 |
|  |  | PROGRAM<br>ELEMENT NO  | PROJECT<br>NO  | TASK<br>NO | WORK UNIT<br>NO |
| 11 TITLE (Include Security Classification) Energy Deposition<br>in Microvolumes of Silicon From High Energy  |  | 61102F   | 2306   | .13        | 01              |
| 12 PERSONAL AUTHOR(S) Proton Reactions   |  | John N. Bradford   |  |            |                 |
| 13a TYPE OF REPORT<br>In-House Report  | 13b TIME COVERED<br>FROM _____ TO _____    | 14 DATE OF REPORT (Yr., Mo., Day)<br>1984 February   | 15 PAGE COUNT<br>25  |            |                 |
| 16 SUPPLEMENTARY NOTATION  |  |  |  |            |                 |
| 17 COSATI CODES  |  |  | 18 SUBJECT TERMS (Continue on reverse if necessary and identify by block number)<br>Microdosimetry Nuclear reaction<br>Geometrical probability Energy deposition<br>High energy proton Silicon |            |                 |
| FIELD  | GROUP                                      | SUB GR   |  |            |                 |
|  |  |  |  |            |                 |
|  |  |  |  |            |                 |
| 19 ABSTRACT (Continue on reverse if necessary and identify by block number)<br>Energy deposition by reaction secondaries issuing from high energy proton-silicon nucleus reactions is calculated. The basis of the calculation formalism is geometrical probability and follows from a direct analogue in radiobiology. Chord length (Track Segment Length), differential, and integral energy deposition distribution functions are calculated along with the first two moments of the distributions. The results enable description of energy deposition in microvolumes of silicon, for example, micro-electronic memory cells. 4 |  |  |  |            |                 |
| 20 DISTRIBUTION AVAILABILITY OF ABSTRACT<br>UNCLASSIFIED UNLIMITED <input checked="" type="checkbox"/> SAME AS RPT <input type="checkbox"/> DTIC USERS <input type="checkbox"/>  |  | 21 ABSTRACT SECURITY CLASSIFICATION<br>Unclassified  |  |            |                 |
| 22a NAME OF RESPONSIBLE INDIVIDUAL<br>John N. Bradford   |  | 22b TELEPHONE NUMBER<br>(Include Area Code)<br>(617)861-4053   | 22c OFFICE SYMBOL<br>ESR   |            |                 |

DD FORM 1473, 83 APR

EDITION OF 1 JAN 73 IS OBSOLETE

Unclassified  
SECURITY CLASSIFICATION OF THIS PAGE

## Contents

|       |  |    |
|-------|--|----|
| 1.    | INTRODUCTION   | 5  |
| 2.    | FORMALISM FOR ENERGY DEPOSITION FROM NUCLEAR REACTION SECONDARIES        | 5  |
| 2.1   | Secondaries Produced Outside the Collection Volume                       | 6  |
| 2.2   | Secondaries Produced Inside the Collection Volume                        | 7  |
| 2.3   | Total Production   | 8  |
| 2.4   | Differential Energy Deposition Spectra; Event Spectra                    | 8  |
| 3.    | SUMMATION OF THE INDIVIDUAL EVENT SPECTRA                                | 10 |
| 3.1   | Convolution  | 10 |
| 3.2   | Weighting of Spectra   | 11 |
| 3.2.1 | Heavy Particles  | 12 |
| 3.2.2 | Coincidence With Light Particles   | 14 |
| 4.    | REACTION SPECTRA   | 15 |
| 5.    | RESULTS AND DISCUSSION   | 16 |
| 6.    | VALIDITY - EXTENSION TO VERY SMALL SIZES AND VERY LOW THRESHOLD ENERGIES | 22 |
| 7.    | COMPUTER CODE EDPMON   | 24 |
|       | REFERENCES   | 25 |

**S** DTIC  
 ELECTE  
 AUG 21 1984  
**D**  
 B

|                    |                                     |
|--------------------|-------------------------------------|
| Accession For      |                                     |
| NTIS GRA&I         | <input checked="" type="checkbox"/> |
| DTIC TAB           | <input type="checkbox"/>            |
| Unannounced        | <input type="checkbox"/>            |
| Justification      |                                     |
| By _____           |                                     |
| Distribution/      |                                     |
| Availability Codes |                                     |
| Dist               | Avail and/or<br>Special             |
| A-1                |                                     |



## Illustrations

|     |  |    |
|-----|--|----|
| 1.  | The Four Classes of Secondary Particles Identified by Their Origin and Path  | 10 |
| 2.  | Energy Deposition Spectra of Neon and Alpha Particle Reaction Products   | 11 |
| 3.  | The Source Volume, $V_u$ , for any Secondary is Bounded by a Parallel Surface Located at a Distance $u$ Range Outside the Collection Volume, $V_o$ | 13 |
| 4.  | The Probability of Energy Deposition Greater Than $\Delta E$ for a Variety of Secondary Species and for Four Collection Volumes                    | 17 |
| 5.  | Energy Deposition Profiles From the Proton Secondaries   | 18 |
| 6.  | Event Spectra From Neon Recoils for Two Volume Sizes   | 19 |
| 7.  | Event Spectra for "Outside Born" Neon Particles and for "Inside Born" for Two Volume Sizes   | 20 |
| 8.  | Weighted $C^{12}$ and Coincidence Event Spectra, With Weighting Fractions Determined by the Procedure Detailed in the Text                         | 21 |
| 9.  | Grand Summation for Events Greater Than $\Delta E$ for High Energy Proton (100 MeV to 1 GeV) Reaction Products in Silicon                          | 22 |
| 10. | Domain Diagram for Contributions to the Variance of the Event Spectra  | 23 |

## Table

|    |                                 |    |
|----|---------------------------------|----|
| 1. | Spectra of Secondary Population | 16 |
|----|---------------------------------|----|

# Energy Deposition in Microvolumes of Silicon From High Energy Proton Reactions

## 1. INTRODUCTION

The production of circuit upsets and logic errors by passage of highly ionizing particles such as cosmic rays or alpha particles through microelectronic circuitry has been under investigation for more than five years.<sup>1-10</sup> The analyses of these events are based on the probability of a particle possessing sufficient energy and stopping power, and the probability that the particle has a track segment (chord length) in the collection volume long enough to deposit the required energy for upset. The charges liberated by the energy deposition are then collected as a pulse or on a storage node to cause a soft error. In this report, the ionizing particles are assumed to be created by the inelastic scatter and reactions of protons in the energy range from 100 MeV to 1 GeV with Si<sup>28</sup> nuclei. Much of the background for this work and some results are in the literature and are not repeated here.

## 2. FORMALISM FOR ENERGY DEPOSITION FROM NUCLEAR REACTION SECONDARIES

When describing the energy deposition by nuclear reaction secondaries in a prescribed convex volume  $V$ , one must account for three features: (1) the stopping

---

(Received for publication 25 January 1984)

(Due to the large number of references cited above, they will not be listed here. See References, page 25.)

power is energy dependent and is variable along the track; (2) the range of the particle is finite; (3) the particles are made locally, that is, production occurs both inside and outside the collection volume, and both locations contribute. The formalism assumes that the secondaries are in bulk equilibrium (the spectrum is spatially independent).

## 2.1 Secondaries Produced Outside the Collection Volume

The number of secondaries of a particular species produced by incident primary radiation (for example, protons) interacting with the host nucleus through a cross section  $\sigma$  is given by

$$\phi' = \Phi \sigma \frac{N}{A} \phi(E) \quad (1)$$

where  $\Phi$  is the primary flux in protons/cm<sup>2</sup>,  $\sigma$  is the total cross section in (cm<sup>2</sup>/host atom · proton) for the particular species,  $N/A$  is the number of host atoms/gm, and  $\phi(E)$  is the frequency distribution (probability density) for secondaries of energy  $E$ , in secondaries/MeV. These dimensions result in  $\phi'$  being given in units of (secondaries/gm · MeV).

The bulk equilibrium flux that results is given by

$$\frac{N'(E) \text{ particles}}{\text{cm}^2 \cdot \text{MeV}} = \frac{\int_0^{E_{\max}} \phi'(E') dE'}{\frac{1}{\rho \text{ gm/cm}^3} L_T(E) (\text{MeV/cm})} \quad (2)$$

where  $\rho$  is the host density and  $L_T(E)$  is the total Linear Energy Transfer (LET).

A convex surface of  $S \text{ cm}^2$  that bounds a volume immersed in an isotropic flux of  $N'(E)$  particles will intercept

$$N'(E) S/4 \text{ particles} . \quad (3)$$

The probability of these lying along a track (chord) length greater than or equal to the length required to deposit  $\Delta E_{\text{threshold}}$  is given by  $C(s[E, \Delta E])$ . The function  $C(s)$  is described in detail in Reference 6.

Hence, the number of energy depositions greater than  $\Delta E_{\text{th}}$  from reactions occurring outside the collection volume is given by:

$$n(\Delta E_{\text{th}}) = \int_{\Delta E_{\text{th}}}^{E_{\max}} N'(E) \frac{S}{4} C(s[E, \Delta E_{\text{th}}]) dE$$

$$= \int_{\Delta E_{th}}^{E_{max}} \Phi \sigma \frac{N}{A} \rho \frac{S}{4} C(s|E, \Delta E) \frac{\int_E^{E_{max}} \phi(E') dE'}{L_T(E)}, \quad (4)$$

and finally, using the Cauchy value for mean chord length,  $\bar{L} = 4V/S$

$$n(\Delta E_{th}) = \int_{\Delta E_{th}}^{E_{max}} \Phi \sigma \frac{N}{A} \rho \frac{V}{\bar{L}} C(s|E, \Delta E) N(E) dE \quad (5)$$

where  $N(E)$  is given by

$$N(E) = \frac{\int_E^{E_{max}} \phi(E') dE'}{L_T(E)} \quad (6)$$

and has the normalization

$$\int_0^{E_{max}} N(E) dE = \bar{u} \text{ (mean range) .}$$

Thus, the maximum value obtainable by Eq. (5) is

$$n(\Delta E_{th} = 0) = \Phi \sigma \frac{N}{A} \rho \frac{V}{\bar{L}} \bar{u}. \quad (7)$$

## 2.2 Secondaries Produced Inside the Collection Volume

The number of secondaries produced in a volume  $V$  by the same incident flux of primaries is given by

$$\phi'(E) = \Phi \sigma \frac{N}{A} \rho V \phi(E) \text{ particles/MeV} \quad (8)$$

and the probability of lying on an internal path segment  $s$  of sufficient length to deposit  $\Delta E_{th}$  or greater is given by  $G(s|E, \Delta E)$ . Hence, the number of energy depositions greater than  $\Delta E_{th}$  due to reactions inside the collection volume is given by

$$n(\Delta E_{th}) = \Phi \sigma \frac{N}{A} \rho V \int_{\Delta E_{th}}^{E_{max}} G(s|\Delta E, E) \phi(E) dE. \quad (9)$$

$G(s)$  is described in detail in Reference 6. The maximum value obtainable by Eq. (9) is  $n(0) = \Phi \sigma \frac{N}{A} \rho V$ .

### 2.3 Total Production

The total number of energy depositions greater than  $\Delta E_{th}$  is given by the sum of Eqs. (5) and (9).

$$n_T(\Delta E) = \Phi \sigma \frac{N}{A} \rho V \left[ \frac{1}{\ell} \int_{\Delta E_{th}/g}^{E_{max}} C(s[E, \Delta E]) N(E) dE \right. \\ \left. + \int_{\Delta E_{th}/g}^{E_{max}} G(s[E, \Delta E]) \phi(E) dE \right] . \quad (10)$$

The chord length required to deposit  $\Delta E$  is determined from

$$s = \int_E^{E-\Delta E} \frac{1}{L(E^*)} dE^* \quad (11)$$

where  $L(E^*)$  is the electronic stopping power.

In the lower limit of the integrals in  $n_T$  a factor  $g$  has been introduced. This function is required for ions other than protons because at low energies ( $E < 10$  keV/nucleon) the electronic stopping power begins to decline and atomic scattering becomes the chief energy loss mode. Thus, if an amount of energy  $\Delta E_{th}$  is required as ionizing energy deposition, an initial kinetic energy of  $\Delta E_{th}/g$  is needed.

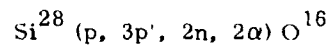
From the work of Sattler the  $g$  factor in silicon is taken as

$$g = \left( 1 - \frac{0.1A}{7} e^{-20\Delta E/A} \right) \quad (12)$$

where  $A$  is the mass number of the particle.

### 2.4 Differential Energy Deposition Spectra: Event Spectra

The inelastic scatter of high energy protons from silicon causes reactions in which several secondary particles are emitted. By way of example the reaction



involves eight outbound particles of which six are charged. Each of these has an energy deposition spectrum. The particles are created "simultaneously" and therefore the total energy deposition is seen as a single event. Thus, to create the correct total energy deposition spectrum one must first determine the individual

event spectra and then combine them in an appropriate way. To do this one needs the differential of the  $n_T(\Delta E)$ , Eq. (10):

$$\begin{aligned} \frac{-\partial n_T(\Delta E)}{\partial \Delta E} = & \Phi \sigma \frac{N}{\Lambda} \rho V \left[ \frac{1}{\bar{l}} \int_{\Delta E/g}^{E_{\max}} \frac{f(s)N(E) dE}{L_e(E - \Delta E)} \right. \\ & + \frac{1}{\bar{l}} C \{s(\Delta E/g)\} N(\Delta E/g) \frac{\partial(\Delta E/g)}{\partial \Delta E} + \int_{\Delta E/g}^{E_{\max}} \frac{C(s[E, \Delta E]) \phi(E) dE}{\bar{l} L_e(E - \Delta E)} \\ & \left. + G \{s(\Delta E/g)\} \phi(\Delta E/g) \frac{\partial(\Delta E/g)}{\partial \Delta E} \right] \end{aligned} \quad (13)$$

where we have used

$$\frac{\partial s}{\partial \Delta E} = \frac{\partial}{\partial s} \frac{\partial s}{\partial \Delta E}$$

and

$$\frac{\partial s}{\partial \Delta E} = \frac{1}{L_e(E - \Delta E)}.$$

The separate terms have been labeled by Caswell<sup>11</sup> as Crossers, Stoppers, Starters, and Insiders. Crossers are particles born outside the collection volume which transit completely through the collection volumes. Crossers are the dominant population wherever the  $\bar{l}$  of the volume is small compared to the mean range of the secondary.

Stoppers are particles born outside the collection volume whose residual track length upon arrival at the surface is shorter than the chord length along which the track lies. Hence, the particle track terminates in the interior of the collection volume and the energy dump equals the total kinetic energy.

Starters are particles born inside the collection volume whose range is greater than the chord segment length to the surface. Hence, they escape the collection volume.

Insiders are particles born inside the collection volume whose range is shorter than the chord segment to the surface. Hence, the particle's entire track is in the interior and the energy dump equals the total kinetic energy. These four classes of particles are shown in Figure 1.

11. Caswell, R. S., and Coyne, J. J. (1975) Microdosimetric spectra and parameters of fast neutrons, Fifth Symposium on Microdosimetry, Verbania Pallanza, Italy, J. Booz, H. G. Ebert, and B. G. R. Smith, Eds., Commission of the European Communities, Luxembourg, EUR 5452 d-f-e, p. 97.

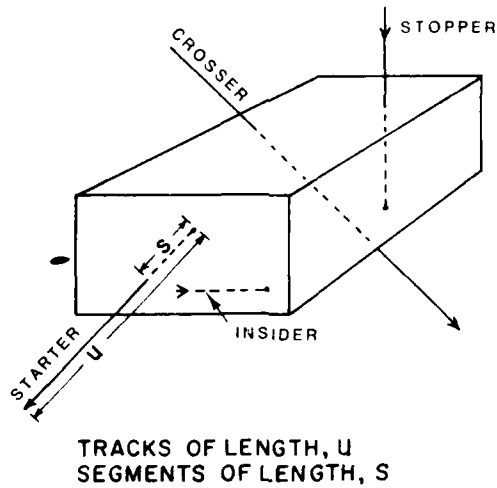


Figure 1. The Four Classes of Secondary Particles Identified by Their Origin and Path

### 3. SUMMATION OF THE INDIVIDUAL EVENT SPECTRA

#### 3.1 Convolution

The mathematical procedure for combining independent spectra is called convolution. The independent event spectra are normalized to unity and represent proper probability densities or frequency functions. The formal rule for combination is

$$n(\delta) = \int_0^{(\Delta E_1 + \Delta E_2)_{\max}} n_1(\Delta E) n_2(\delta - \Delta E) d\Delta E \quad (14)$$

where the  $n_1$  are the independent spectra. Caution is necessary since different spectra will usually have different ranges. Therefore, Eq. (14) must be divided into two parts

$$n(\delta) = \int_0^{\delta} n_1(\Delta E) n_2(\delta - \Delta E) d\Delta E \quad (15)$$

$$0 < \delta < \Delta E_{1\max}$$

$$n(\delta) = \int_0^{(\Delta E_1 + \Delta E_2)_{\max}} n_1(\Delta E) n_2(\delta - \Delta E) d\Delta E$$

$$\Delta E_{\max} < \delta < (\Delta E_1 + \Delta E_2)_{\max} . \quad (16)$$

Note that the spectrum with the least range takes the role of  $n_1$  in the integral. If there is a third particle, a second convolution must be performed.

This is the procedure which is applied directly to the particles of inside production. The starters and insiders spectra from Eq. (13) are added and convolved with those from the second particle. An example of the resulting spectrum is shown in Figure 2.

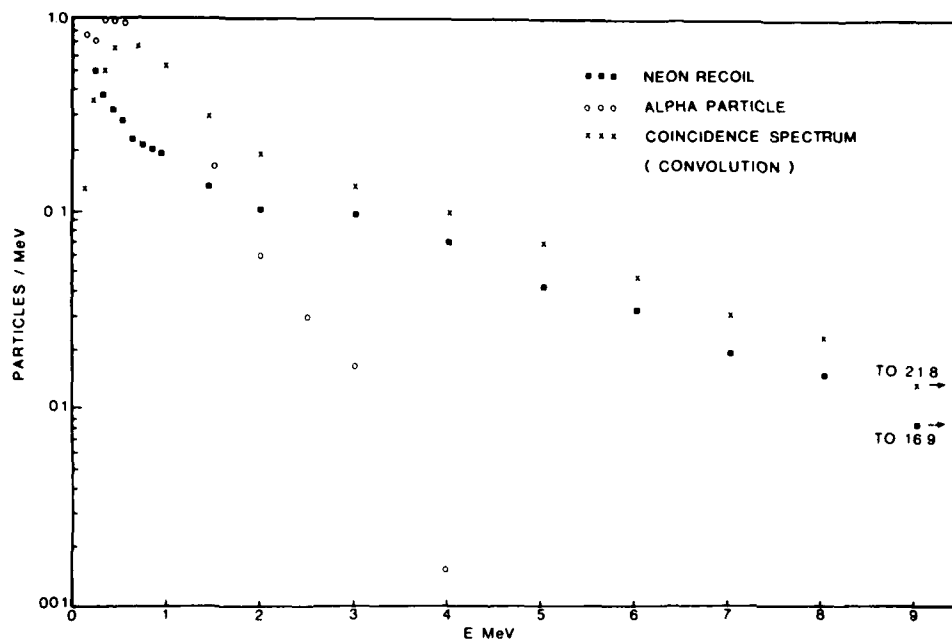


Figure 2. Energy Deposition Spectra of Neon and Alpha Particle Reaction Products. The coincidence spectrum obtained by convolution is also shown

### 3.2 Weighting of Spectra

The microvolume of the electronic device that collects the charge acts very much like a detector. One can treat the total energy event spectrum as the sum of several input spectra, each of these being identified by its origin. One such is the

spectrum that arises from reactions in the interior; this spectrum is obtained by the convolution process above. From reactions that occur outside the microvolume, several additional spectra are created.

In the example reaction above, an  $0^{16}$  recoil is produced with three protons and two alpha particles. A spectrum arises from each of these plus a spectrum for each coincidence, double coincidence and so forth. The procedure is to establish each of these energy deposition spectra by the convolution process and to assign a weighting factor  $\gamma$  to each where the value of  $\gamma$  is determined by the relative probability of its occurrence.

To determine a general rule for assigning a value of  $\gamma$  one can proceed as follows:

### 3.2.1 HEAVY PARTICLES

The total number of reactions that occur outside the volume and whose heavy recoils have range large enough to reach the collection volume so as to deposit some energy is given by

$$n = \Phi \sigma_u \frac{N}{A} \rho [V_u - V_o] \quad (17)$$

for recoils of range  $u$ , and where  $V_u$  is the volume enclosed by a surface parallel to  $V_o$  at distance  $u$ . For a spectrum of particles the probability of range  $u$  is  $r(u)$  so

$$n = \Phi \sigma \frac{N}{A} \rho \int_0^{u_{\max}} (V_u - V_o) r(u) du . \quad (18)$$

For each  $u$  value one must determine the probability of a recoil hitting the collection volume. To do this exactly one would have to calculate the probabilities from a Monte Carlo geometry program. However, since the results are to be integrated twice over, it is reasonable and of sufficient accuracy to use mean values and the following approximation.

Consider the collection volume  $V_o$  and around it the source volume  $V_u - V_o$  as shown in Figure 3. Between  $V_u$  and  $V_o$  create the parallel surface at distance  $x$ . The probability of a reaction secondary originating in this shell is

$$\frac{S(x) dx}{V_u - V_o} .$$

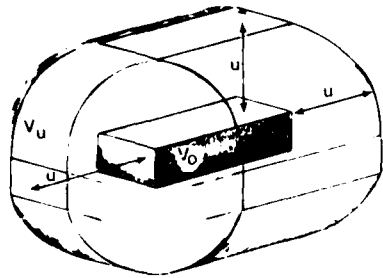


Figure 3. The Source Volume  $V_u$  for any Secondary is Bounded by a Parallel Surface Located at a Distance  $u =$  Range Outside the Collection Volume,  $V_o$

PARALLEL SURFACE - SOURCE VOLUME

From geometric probability one knows that the probability of one of  $u$  random infinite lines hitting  $V_o$ , if the line hits  $S(x)$ , is given by the ratio of the surface areas,  $S_o/S(x)$ .

Here, the ranges are finite and oriented, which means one must modify this probability by multiplying by a function of  $(x, u)$  to account for the finite range and directedness. We obtain

$$f(x, u) S_o / 2S(x)$$

where the factor of 2 accounts properly for the directedness of the track. We obtain by insertion into Eq. (18)

$$n = \Phi \sigma \frac{N}{A} \rho \int_0^{u_{\max}} (V_u - V_o) r(u) \int_0^u \frac{S_o}{2S(x)} f(x, u) \frac{S(x) dx du}{V_u - V_o}. \quad (19)$$

The boundary conditions on  $f(x, u)$  are:

- (1)  $f(x, u) \rightarrow 1$  at  $x = 0$
- (2)  $f(x, u) \rightarrow 1$  as  $u \rightarrow \infty$
- (3) To get Eq. (7) from Eq. (19) one must have

$$\int_0^u \left( \frac{S_o}{2S(x)} \right) f(x, u) \frac{S(x)}{V_u - V_o} dx = \frac{S_o u/4}{V_u - V_o}$$

that is,

$$\int_0^u f(x, u) dx = u/2.$$

Solutions which obey this condition include

- (1)  $f(x, u) = 1 - x/u$
- (2)  $= (1 - x/u) + x/u(1 - x/u) (1 - 2x/u)$
- (3) Power series in  $(1 - x/u) x/u$ .

We have used Solutions 1 and 2 and chosen Solution 1 as sufficiently accurate. Solution 3 yields nearly identical results to Solution 2. Insertion into Eq. (19) yields the number of recoils that are crossers and stoppers.

### 3.2.2 COINCIDENCE WITH LIGHT PARTICLES

Since the range of the light particles is so much greater than that of the recoils, their range  $u$  can be treated as an infinite line. Hence the probability of light particle intercept is

$$\frac{S_o}{2S(x)}.$$

The coincidence probabilities of  $n$  particles scoring  $m$  hits are then binomially distributed in this factor:

$$\left\{ \binom{n}{m} \left( \frac{S_o}{2S(x)} \right)^m \left( 1 - \frac{S_o}{2S(x)} \right)^{n-m} \right\}. \quad (20)$$

Thus, insertion of Eq. (20) into Eq. (19) yields the number of coincidences. The ratio of that number to the total number of particles gives the weighting factor. Since the sum of all the coincidences (including 0<sup>th</sup>) equals the total number of particles it is equivalent to normalize the weighting by dividing by their sum. We obtain

$$\gamma_{\text{raw}}^n = \int_0^{u_{\text{max}}} r(u) \int_0^u \frac{S_o}{2S(x)} f_1(x, u) \left\{ \frac{n}{m} \left( \frac{S_o}{2S(x)} \right)^m \left( 1 - \frac{S_o}{2S(x)} \right)^{n-m} \right\} R(x)^m dx du \quad (21)$$

The factor  $\Phi \sigma_A^N \rho$  is dropped since it is common to all  $\gamma_m^n$ . The factor  $R(x)^m$  is the range sum distribution and is the probability of the light particle range being greater than  $x$  [this insures the possibility of coincidence].

The mixing ratios of weighting factors for each spectrum are then determined by normalizing to the sum of the  $\gamma_m^n$ :

$$\gamma_m^n = \frac{\gamma_m^n \text{ raw}}{\sum \gamma_m^n} . \quad (22)$$

Thus, in a reaction which produces  $n$  light particles and a heavy recoil, the coincidence spectrum for  $m^{\text{th}}$  order coincidence (convolution) is weighted by  $\gamma_m^n$ .

#### 4. REACTION SPECTRA

The secondary spectra from high energy proton reactions are generated by codes developed by high energy physics groups. The code used to generate the spectra given later in this report is the Medium Energy Collision Cascade Code-7 at Oak Ridge National Laboratory. The work was performed under contract RADC-2306J320. Other codes exist which are suitable, that is, they produce reaction secondary energy spectra and cross sections. The most notable is probably the HETC code of Chandler and Armstrong.

The output of the codes are differential spectra in energy and angle. The formalism of chord length demands isotropic fluxes so we presume isotropic angular distribution and the integrated spectra (a good approximation) over angles.

The output of a specific case, a 400 MeV proton on  $\text{Si}^{28}$ , is illuminating:

- (1) There are 70 (A, Z) products.
- (2) The total inelastic cross section is 420 mB.
- (3) The individual (A, Z) cross sections range from 0.01 mB (several) to (27, 14) 54 mB.
- (4) There are evaporation spectra for the light particle production,  $p, n, d, N_e^3, H_e^4$ .
- (5) Thirteen of the (A, Z) secondaries contain 82 percent of the total cross section. These may be combined by isotopes to yield eight spectra sufficient to characterize all the spectra.
- (6) The cross sections for incident protons with energies from 100 MeV to 1 GeV are slowly varying, making average calculations meaningful for this whole energy domain. This domain constitutes the essence of the cosmic ray background flux.

The eight spectra that characterize this entire secondary population are listed in Table 1.

Table 1. Spectra of Secondary Population

| A              | Z  | $\bar{A}$ | $\sigma$ mB | Convolution Products |
|----------------|----|-----------|-------------|----------------------|
| 28, 27         | 14 | 27        | 73          |                      |
| 25, 26, 27     | 13 | 26        | 114         | 1p                   |
| 23, 24, 25, 26 | 12 | 24        | 114         | 2p                   |
| 22, 23, 24     | 11 | 23        | 62          | $\alpha$ , p         |
| 20, 21, 22     | 10 | 21        | 44          | 2p, $\alpha$         |
| 16             | 8  | 16        | 24          | 2 $\alpha$ , 2p      |
| 14             | 7  | 14        | 22          | 2 $\alpha$ , 3p      |
| 12             | 6  | 12        | 12          | 3 $\alpha$ , 2p      |

## 5. RESULTS AND DISCUSSION

Two features of the ionizing energy deposition in microelectronics are worthy of further mention. These are (1) the notion of the collection volume and (2) the charge collection mechanism that follows the deposition.

(1) In the mathematics of geometrical probability the collection volumes are required to be convex and are taken to be right rectangular volumes. The difficulty arises in the determination of the size (dimensions) of the volume since several transport/collection processes are at work. These are: strong field collection within the depletion zone, diffusion into the collection volume, and plasma column or "funnel" effects. The chord length-LET mode of analysis does not explicitly treat the second two of these processes and one can only adjust the dimensions of the collection volume in an ad hoc way to correct for them. To date the determination of the collection volume dimensions remains an imprecise factor but they are generally taken as the lateral dimensions of the n+ collector implant plus a diffusion length and the depletion depth.

(2) The connection between energy deposition in the form of electron-hole pairs and the charge ( $Q_{crit}$ ) required to represent an error is provided through the relation:

$$\Delta E_{threshold} = \frac{Q_{crit}(\text{coulombs}) W (\text{eV e-h pair})}{e (\text{coulombs/electron}) \bar{\eta}}$$

where  $W = 3.6$  eV in silicon and  $\bar{\eta}$  is the mean collection efficiency for a charge created in the collection volume. This relationship represents a point of departure between two possible modes of analysis:

- (a) An analysis based on isotropic fluxes of secondary particles with appropriate chord length probabilities. This approach necessarily averages over initial charge location and hence utilizes  $\bar{z}$ .
- (b) A specific track by track Monte Carlo analysis which details the position of electrons and holes and collects them via local fields to produce  $Q_{crit}$ . The difficulty with this approach is that it requires enormous amounts of computation, and these intermediate results, in the final analysis, must be averaged to produce an estimate of a circuit response.

This report describes the energy deposition in small volumes (micron dimensions) based on approach (a) above in the hope that the loss of detail in the generality of the method is made up by wider applicability.

Solutions to Eq. (10), which gives the event rate for recoils, are shown in Figure 4. For each volume there is great commonality in the event rate for all

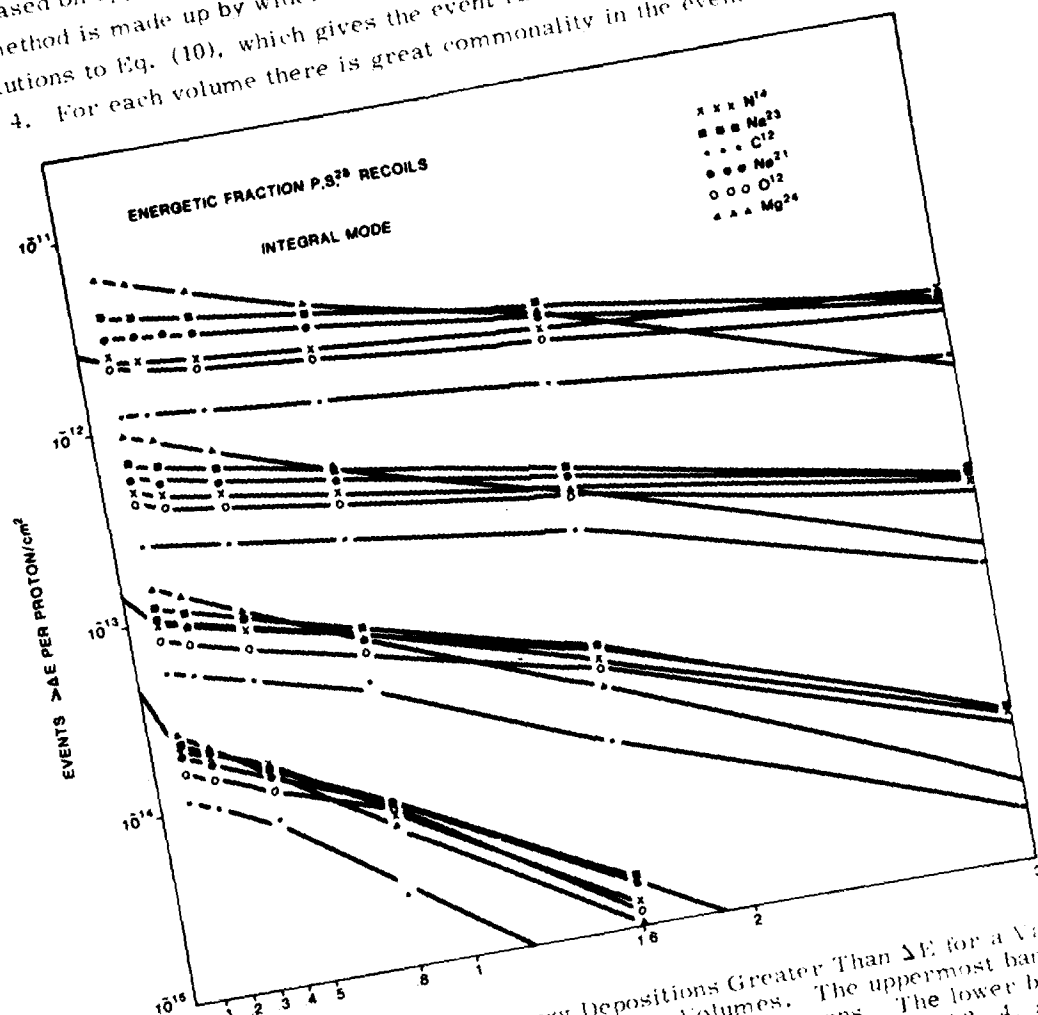


Figure 4. The Probability of Energy Depositions Greater Than  $\Delta E$  for a Variety of Secondary Species and for Four Collection Volumes. The uppermost band is for a volume whose dimensions are  $3.5 \times 14 \times 21$  microns. The lower bands are for volumes whose dimensions have been reduced by a factor of 2, 4, and 8 respectively.

species. The difference in rates can be traced largely to the difference in cross section for species production. The solution to Eq. (10) for the proton evaporation spectrum is shown in Figure 5. No curve is shown for the largest volume since the proton energy deposition is too small to be of consequence. As these curves show, large numbers of proton-generated energy depositions take place but are so small in value as not to contribute to the soft error rate (dashed line).

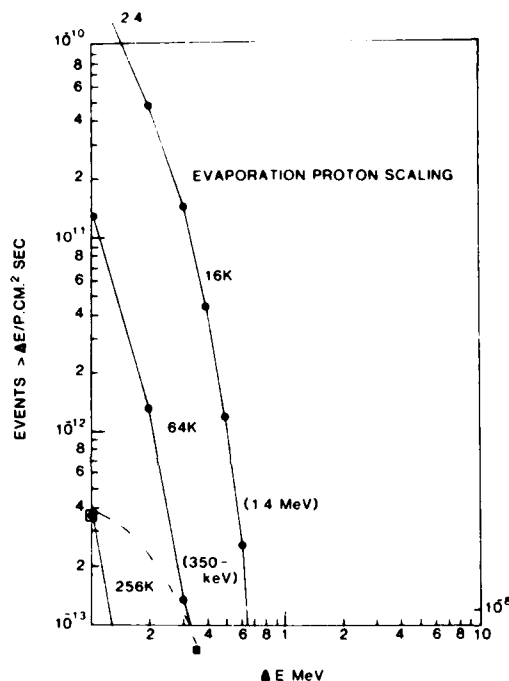


Figure 5. Energy Deposition Profiles From the Proton Secondaries. Although large in number, the profiles are concentrated at very low  $\Delta E$  values and so do not contribute greatly to single event upset until 256 K RAM size arrays

The solution to Eq. (13), the event spectrum or differential energy loss spectrum, for neon is shown in Figure 6. The two cases displayed, the largest and smallest volumes treated, show the considerable range of probability for energy deposition. In spite of this the mean  $\Delta E$  for the large volume is only 3.6 MeV, not enough to trigger electronic upset ( $\Delta E_{th} = 5.6$  MeV).

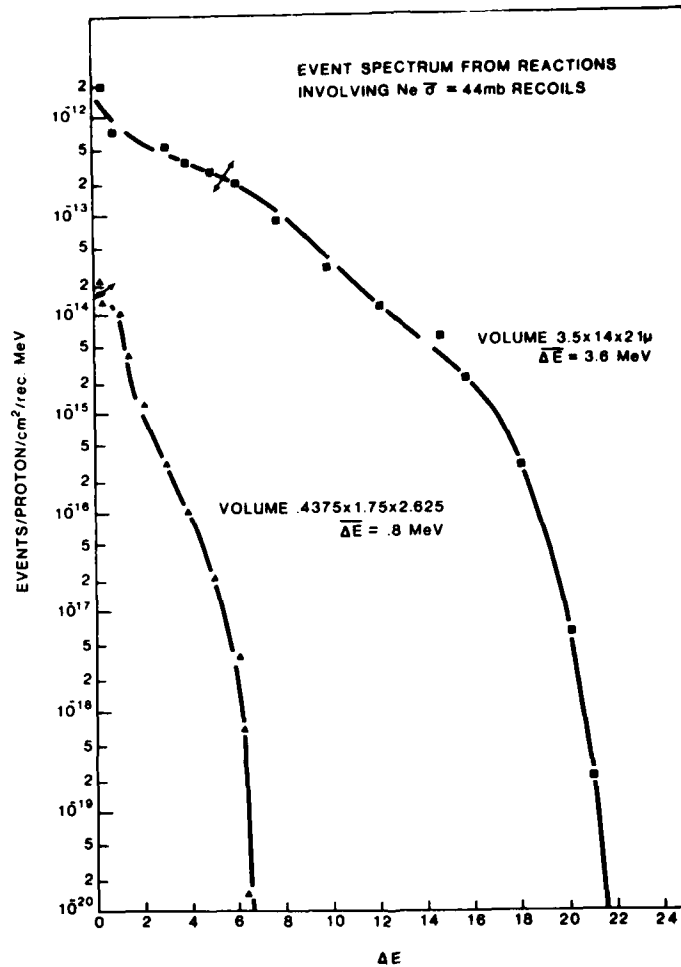


Figure 6. Event Spectra From Neon Recoils for Two Volume Sizes. Arrows indicate threshold energy required for nominal device upset

As explained above, the particles and their energy deposition can be identified by their origin: outside the volume or inside. The relative contribution from each source for the neon recoil reactions can be seen in Figure 7 for the largest and smallest volume. In the large volume the contributions are dominated by inside production. This occurs because the mean range  $\bar{u}$  for neon is less than the mean chord length  $\bar{l}$ :  $\bar{u}_{\text{Ne}} = 3.6 \text{ u}$ ,  $\bar{l}_{\text{larger}} = 5 \text{ u}$ . In the limiting form the contributions of outside to inside productions approach  $\bar{u}/\bar{l}$  to 1. This effect shows clearly in the small box where outside production dominates. Here  $\bar{l}_{\text{small}} = 1.25 \text{ u}$ .

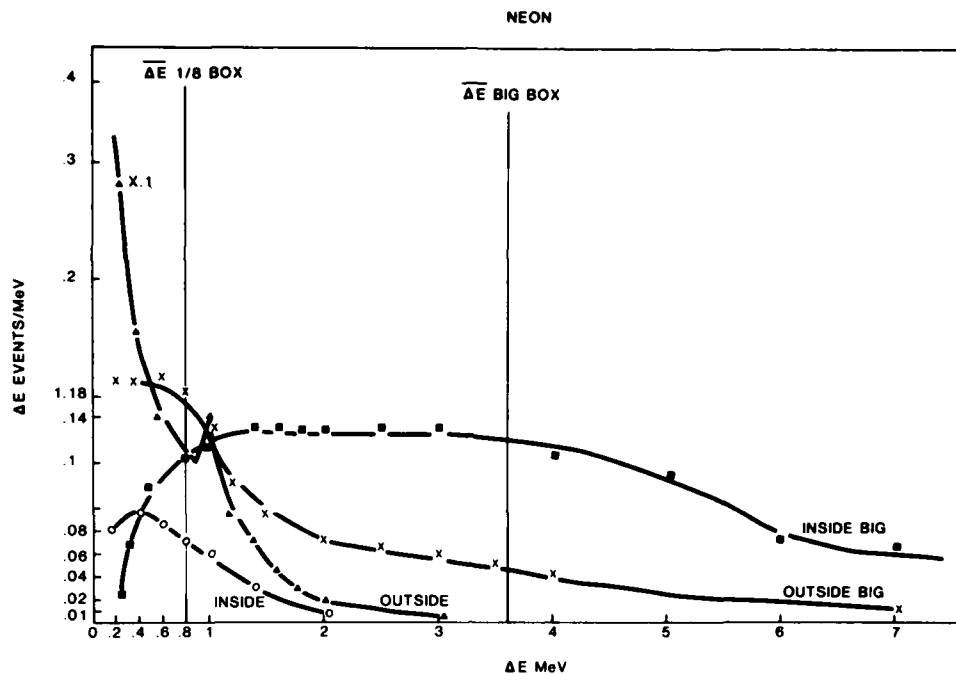


Figure 7. Event Spectra for "Outside Born" Neon Particles and for "Inside Born" for Two Volume Sizes. Inside production dominates large volumes, outside dominates small volumes

One can see the impact of the coincidence  $\alpha$  particles in Figure 8 for those reactions which produce  $C^{12}$  recoils. The weighted spectra show quite similar shapes, each offset due to approximately the mean  $\alpha$  particle  $\Delta E$  contribution. Not shown in the figure is the long high energy tail that results in the 3  $\alpha$  case extending to 33 MeV.

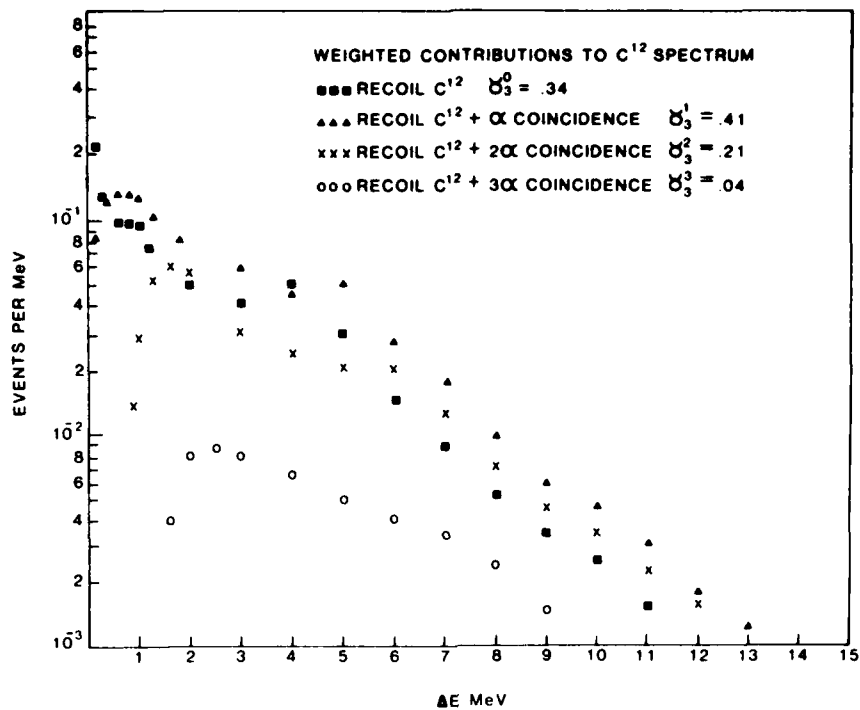


Figure 8. Weighted C<sup>12</sup> and Coincidence Event Spectra, With Weighting Fractions Determined by the Procedure Detailed in the Text

Finally, the complete result of this investigation is shown in Figure 9. This is the grand summation of all contributions. Si inelastic recoils, Al, and Mg recoils, plus the evaporation particles  $\alpha$ , p are added to the coincidence-convolved results for Na, Ne, O, N, and C. An event rate scaling curve is added to show the expected total upset rate. The ordinate has units of upsets per proton per cm<sup>2</sup> per second per cell of volume indicated. The intercept value of  $2.6 \times 10^{-12}$  for the V<sub>0</sub> (4K DRAM) case yields  $\sim 9$  events per year for a 10<sup>5</sup> DRAM. This represents about 5 percent of the observed event rate, the remainder due to heavy cosmic ray ionizing tracks. The plot shows that this event rate declines by a factor of about 3 for the smallest volume. The importance of the scaling law is equally clear. If the decrease in the threshold energy for upset does not follow a  $1/s^2$  (s is the dimension reduction factor) rule but a  $1/s^3$  rule then a dramatic increase in the event rate would occur. Lastly, the resolution of these calculations is 0.1 MeV. Thus, the ultimate domain of VLSI, that with  $\Delta E_{th}$  below 0.1 MeV, is not addressed.

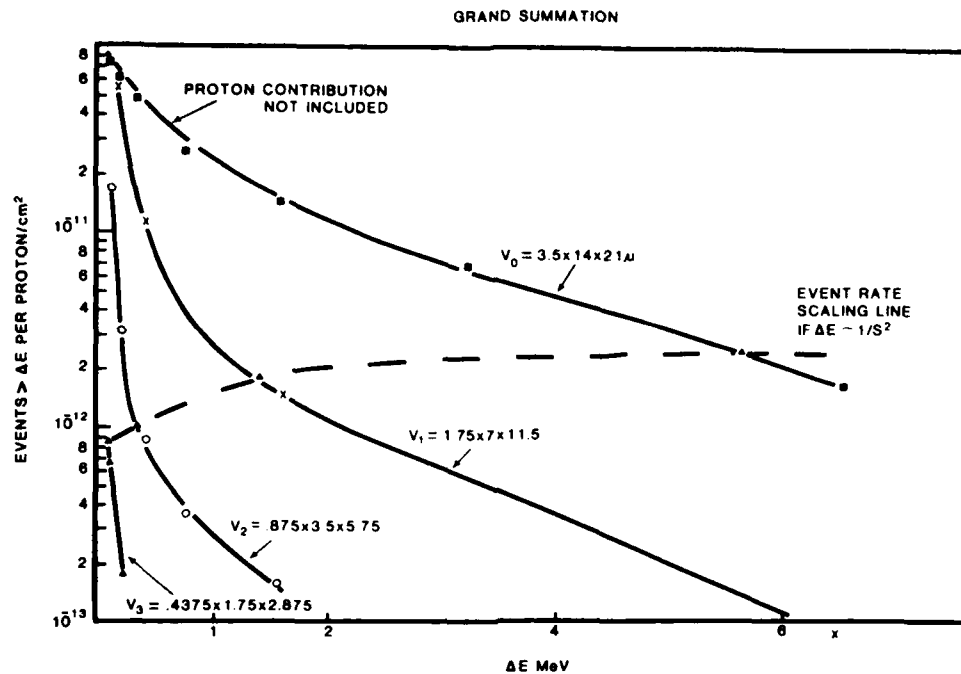


Figure 9. Grand Summation for Events Greater Than  $\Delta E$  for High Energy Proton (100 MeV to 1 GeV) Reaction Products in Silicon. Scaling line intercepts yield event rates

## 6. VALIDITY - EXTENSION TO VERY SMALL SIZES AND VERY LOW THRESHOLD ENERGIES

From the outset, this calculation has been based on the notion that it would be sufficient to characterize the energy deposition and thus upset rates by treating only the major contributions to the variance of the energy deposition distributions. The cosmic ray work was dominated, therefore, by the chord length-LET contribution. In this work, with lower energy particles, it was necessary to include effects of finite range and changing LET (linear energy transfer) along the path in addition. As one proceeds to even smaller dimensions it will become necessary to include two more contributions: (1) delta ray production with a track no longer representable by a line but by a 3-D fuzzy cylinder with large internal gradients; and (2) energy straggling effects.

The entire domain of contribution can be shown on a single diagram. Following the lead of Kellerer and Chmelevsky<sup>12</sup> one can create a figure like Figure 10.

12. Kellerer, A. M., and Chmelevsky, D. (1975) Criteria for the applicability of LET. Rad. Res., 63:226.

These diagrams have neat boundaries only for spherical shapes so I retain those. The ordinate is size (diameter) and the abscissa is energy/nucleon. This diagram is for  $O^{16}$  ions. The domain boundary lines are attempts to show where the effect contributes 10 percent to the variance of the energy deposition.

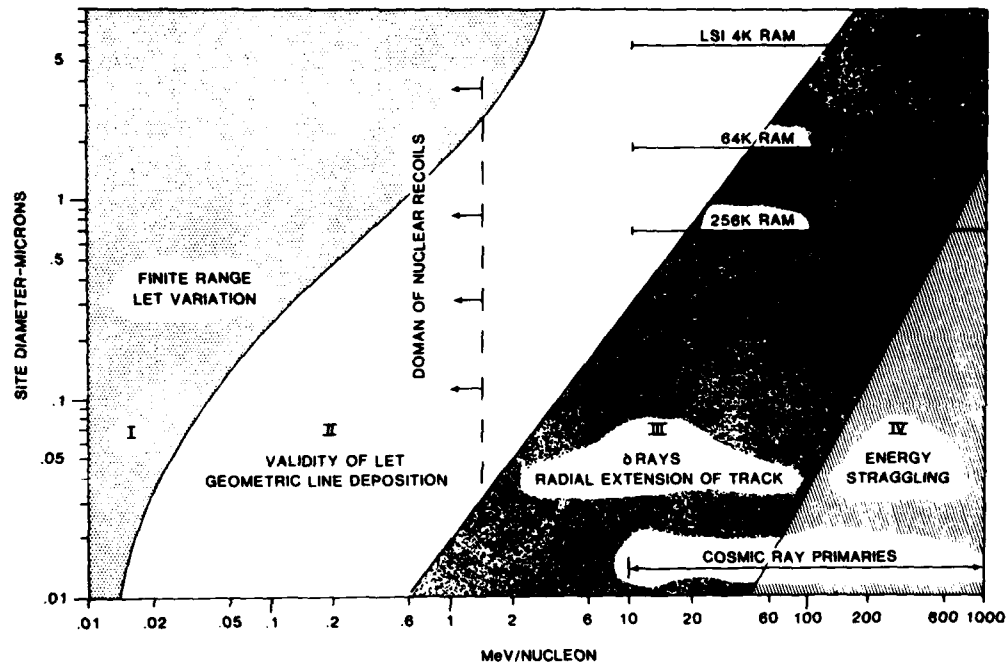


Figure 10. Domain Diagram for Contributions to the Variance of the Event Spectra. Each "boundary" represents ~ 10 percent contribution compared to linear energy transfer chord length contribution

The single event upsets began in a domain of relatively large size and cosmic ray energy, hence upper right on diagram. Sealing and size reduction proceed downward vertically. Inclusion of nuclear reaction secondaries of low energy and finite range spanned domain II and into I. Further size reduction will carry into domain III and IV, delta ray and finite track cross section distribution and energy straggling. This diagram shows that the formalism of this work does not need modification for use in advanced VLSI size domains ( $< 1\mu$ ) but that the cosmic interactions do require a modification to account for the 3-D characteristics of charge distributions around the axis of the track (delta rays) and subsequently to reflect energy straggling.

## 7. COMPUTER CODE EDPMON

The individual computer programs used in these calculations and in foregoing calculations of References 1, 6, and 8 have been combined into one program called EDPMON. This more efficient code was written by Mr. Mark Moses of Bedford Research under USAF Contract F19628-82-C-0139. EDPMON will compute on input of the constants of the problem (1) the chord length distribution functions and first and second moments of the distributions for rectangular volumes, (provision is made to read in chord length tables based on other geometries), (2) the event rate of energy deposition from a single particle species is produced in bulk equilibrium (so called integral mode), (3) the differential energy deposition spectrum for recoil and light secondary particles, (these calculations are performed separately for particles born outside the collection volume and particles born inside the collection volume), (4) coincidence spectra up to triple coincidence (via convolution), and (5) first and second moments of the final energy deposition spectra. An example of a single species run,  $O^{16} \cdot 2\alpha$ , using single and double coincidence, used 306 seconds of Central Processor time.

## References

1. Bradford, J. N. (1978) Heavy Ion Radiation Effects in VLSI, RADC-TR-78-109, AD A061116.
2. Pickel, J. C., and Blandford, J. T. (1978) Cosmic ray induced errors in MOS memory cells, IEEE Trans. Nucl. Sci., NS-25:1166-1171.
3. Ziegler, J. F., and Lanford, W. A. (1979) Effect of cosmic rays on computer memories, Science, 206:776.
4. Guenzer, C. S., Wolicke, E. A., and Atlas, R. G. (1979) Single event upset of dynamic RAMs by neutrons and protons, IEEE Trans. Nucl. Sci., NS-26:5048-5052.
5. Yoney, D. S., Nelson, J. T., and Vanskike, L. L. (1979) Alpha-particle tracks in silicon and their effect on dynamic MOS RAM reliability, IEEE Trans. Elec. Dev., ED-26:10-16.
6. Bradford, J. N. (1979) A distribution function for ion track lengths in rectangular volumes, J. Appl. Phys., 50:3799-3801.
7. Petersen, E. L. (1980) Nuclear reaction in silicon, IEEE Trans. Nucl. Sci., NS-27:1494.
8. Bradford, J. N. (1980) Geometric analyses of soft errors and oxide damage produced by heavy cosmic rays and alpha particles, IEEE Trans. Nucl. Sci., NS-27:942.
9. Petersen, E. L., Shapiro, P., Adams, J. H., Jr., and Burke, E. A. (1982) Calculations of cosmic-ray induced soft upsets and scaling in VLSI devices, IEEE Trans. Nucl. Sci., NS-29:2055-2063.
10. McNulty, P. J. (1983) Charged particles cause microelectronics malfunctions in space, Physics Today, Guest Commentary, 36:9.
11. Caswell, R. S., and Coyne, J. J. (1975) Microdosimetric spectra and parameters of fast neutrons, Fifth Symposium on Microdosimetry, Verbania Pallanza, Italy, J. Booz, H. G. Ebert, and B. G. R. Smith, Eds., Commission of the European Communities, Luxembourg, EUR 5452 d-f-e, p. 97.
12. Kellerer, A. M., and Chmelevsky, D. (1975) Criteria for the applicability of LET, Rad. Res., 63:226.



*MISSION  
of  
Rome Air Development Center*

*RADC plans and executes research, development, test and selected acquisition programs in support of Command, Control Communications and Intelligence (C<sup>3</sup>I) activities. Technical and engineering support within areas of technical competence is provided to ESD Program Offices (POs) and other ESD elements. The principal technical mission areas are communications, electromagnetic guidance and control, surveillance of ground and aerospace objects, intelligence data collection and handling, information system technology, ionospheric propagation, solid state sciences, microwave physics and electronic reliability, maintainability and compatibility.*

10-8

DTI